The Source of the Ti *3d* Defect State in the Band Gap of Rutile Titania (110) Surfaces

K. Mitsuhara[1], H. Okumura[1], A. Visikovskiy[1*], M. Takizawa[2], and Y. Kido[1]

1) Department of Physics, Ritsumeikan University, Kusatsu, Shiga-ken 525-8577, Japan

2) Synchrotron Radiation Center, Ritsumeikan University, Kusatsu, Shiga-ken 525-8577, Japan

Abstract

The origin of the Ti *3d* defect state seen in the band gap for reduced rutile TiO_2(110) surfaces has been excitingly debated. The probable candidates are bridging O vacancies (V_O) and Ti interstitials (Ti-int) condensed near the surfaces. The aim of this study is to give insights into the source of the gap state via photoelectron spectroscopy combined with ion scattering and elastic recoil detection analyses. We have made three important findings; (i) The intensity of the gap state observed is well correlated with the sheet resistance measured with a 4-point probe, inversely proportional to the density of Ti-int. (ii) Sputter/annealing cycles in ultra high vacuum (UHV) lead to efficient V_O creation and condensation of Ti-int near the surface, while only annealing below 870 K in UHV condenses subsurface Ti-int but does not create V_O significantly. (iii) The electronic charge to heal a V_O is almost twice that to create an O adatom adsorbed on the 5-fold Ti row. The results obtained here indicate that both the V_O and Ti-interstitials condensed near the surface region contribute to the gap state and the contribution to the gap state from the Ti-int becomes comparable to that from V_O for the substrates with low sheet resistance less than ~200 Ω/□.

*Present address: *Department of Applied Quantum Physics and Nuclear Engineering, Kyushu University, 744 Motooka Nishi-ku, Fukuoka 819-0395, Japan*

1. Introduction

The origin of the defect state in the band gap seen in ultraviolet photoelectron spectra (UPS) for reduced(*R*-) and hydroxylated(*H*-)TiO_2(110) surfaces has been recently debated excitingly[1-5]. It has been long recognized that the six fold Ti beneath a bridging oxygen (O_{br}) vacancy (V_O) gives the gap state ~0.8 eV below the Fermi level (E_F)[6-8]. It is also known that the defect state has a *d*-state like nature (resonance at 47 eV)[9,10] and thus the Ti^{3+} state which corresponds to a Ti^{4+} core binding one *3d* electron is the most probable candidate[7,10]. Recently, Wendt et al.[1] reported that the Ti *3d* defect state comes from Ti interstitials (Ti-int) segregated near the surface and does not from the V_O. According to the report, exposing an *H*-TiO_2(110) surface with paired $O_{br}H$ to an O_2 gas led to complete disappearance of OH 3σ signal (hybridization of H 1s and O $2p_z$ orbitals) but still kept a strong defect state intensity at low O_2 exposure, indicating existence of a subsurface excess charge (Ti^{3+}: Ti 3d) different from V_O, probably the Ti-int condensed near the surface by annealing in ultrahigh vacuum (UHV)[1,5]. Further exposure to O_2 reduced gradually the defect state intensity owing to donation of the excess charge from Ti-int (Ti^{3+}) to adsorb electronegative species such as O adatoms (O_{ad}) on the 5-fold Ti rows. Figure 1 illustrates a rutile TiO_2(110) surface with V_O, O_{ad}, Ti-int, and paired $O_{br}H$ by a ball and stick model. Quite recently, however, Yim et al.[3] reported based on STM and UPS analysis that the defect state intensity is proportional to the number of V_O created by low energy electron bombardment, which did not change the situation of Ti interstitials near the surface, although they commented that there was a residual charge not related to V_O, probably from Ti-int. Thus the debate on the origin of the defect state still continues.

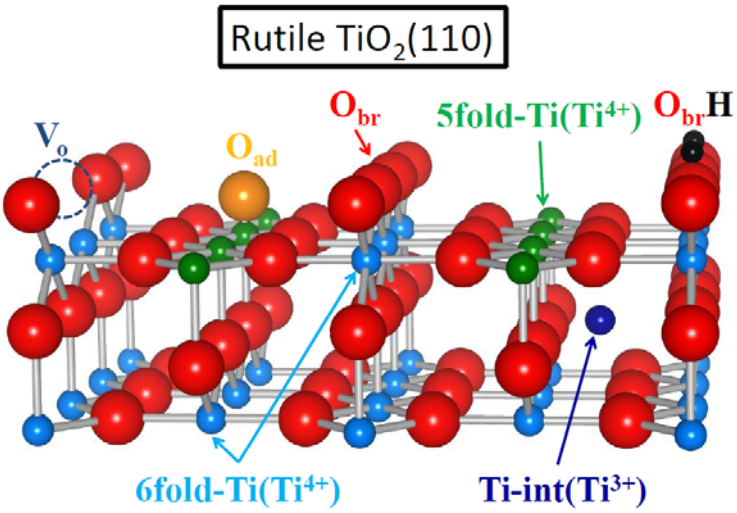

FIG. 1. Ball and stick model of a rutile TiO_2(110) surface with V_O, O_{ad}, Ti-int, and paired $O_{br}H$.

There have been also many efforts to explain the gap state theoretically. Morgan and Watson[8] performed DFT (density functional theory) corrected for on-site Coulomb interaction (GGA+U) for *R*-TiO_2(110) and reproduced the gap state localized on the pairs of 6-fold Ti atoms adjacent to a V_O. According to Valentin and Pacchioni[7], a hybrid exchange functional (B3LYP) also predicted localized gap states; one electron transferred to a 6-fold Ti and another to a 5-fold Ti for both *R*-TiO_2(110) and the *H*-TiO_2(110) surfaces. Recent STM observation, however, revealed the excess charge delocalized and distributed symmetrically on multiple Ti^{4+} sites (5-fold Ti) for both *R*- and *H*-TiO_2(110) surfaces[11]. Sharing of the defect charge by neighboring 5-and 6-fold Ti atoms was also demonstrated by resonant photoelectron diffraction measurements[12]. Concerning the contribution from Ti-int, spin polarized hybrid DFT calculations also showed that a neutral Ti placed in an interstitial site spontaneously transforms into a Ti^{3+} ion with nearly one electron localized on the *3d* shell, which makes the band gap state[13].

In this study, we evaluate quantitatively the contributions from V_O and Ti-int, which may depend on sample preparation conditions by photoemission analysis (UPS and work function) combined with medium energy ion scattering (MEIS) and elastic recoil detection (ERD) using isotopically labeled $^{18}O_2$ and $D_2{}^{18}O$. All the experiments were performed *in situ* under UHV conditions ($\leq 2\times10^{-10}$ Torr) at the beamline-8 named SORIS working at Ritsumeikan SR Center. We measured UPS spectra including the gap state, OH 3σ and Ti 3p and O 2s lines as well as work functions using synchrotron radiation (SR) light. The present MEIS and ERD analyses allow us to derive the absolute amounts (areal densities) of V_O (filled and unfilled V_O) and O_{ad}. Based on the results obtained here, the contributions to the defect state from V_O and other source such as Ti-int are discussed quantitatively. In this regard, it is crucial to estimate the density of Ti interstitials in near-surface regions. We evaluate the density quantitatively by measuring the sheet resistance using a 4-point probe.

2. Experiment

We employed the rutile TiO_2(110) substrates mirror-finished with low enough levels of impurities less than 5 ppm (less than 0.1 ppm for Mg, Ca, Sr, and Ba). Initially the as-supplied TiO_2(110) substrates were annealed at 973 K for 30 min in UHV to be conductive and the color changed into blue from transparency. The reduced surfaces denoted by *R*-TiO_2(110) were prepared by several cycles of 0.75 keV

Ar^+-sputtering and annealing at 870 K for 10 min in UHV finished by the annealing at 870 K for 10 min. The surface showed a clear (1×1) pattern in a reflection high energy electron diffraction (RHEED) image. The reduced surface was cooled down to ~323 K and then dosed with O_2 (5×10^{-6} Torr) for 200 s (1000 L, 1 L = 1×10^{-6} Torr s) continuing the cooling process to room temperature (RT). This led to formation of an O-rich surface denoted by *O*-TiO_2(110), where about half (or slightly less) of the V_O vacancies were filled with O, together with O adatoms adsorbed on the 5-fold Ti rows[14]. The *H*-TiO_2(110) surface was prepared by exposing the *R*-TiO_2(110) to $H_2{}^{16}O$($H_2{}^{18}O$, $D_2{}^{18}O$) at ~330 K. In order to avoid the H_2O adsorption at structural defects such as step edges and kinks, we heated slightly the samples during H_2O exposure.

UPS analysis was performed using SR light at photon energy of 50 and 90 eV under normal emission condition. Photoelectrons were detected with a concentric hemispherical analyzer with a mean radius of 139.7 mm. Taking the photon energy ($h\nu$) of 50 eV is advantageous to detect the Ti 3d defect state most sensitively, while the sensitivity to the OH 3σ is superior at the photon energy of 90 eV. All the UPS spectra were observed at the $[1\bar{1}0]$-azimuth because of the stronger intensity of the Ti *3d* defect state than that at the [001]-azimuth. The photon energy was calibrated with second harmonic waves assuming the binding energy (E_B) of Au $4f_{7/2}$ line to be 84.0 eV. We also measured work functions (Φ) by means of photon-induced secondary ($h\nu = 140$ eV) electron emission from surfaces, which were negatively biased ($-V$)[14]. The work function is given by

$$\Phi = E_{kin}^{0} + \Phi_{SP} - eV \qquad (1)$$

where Φ_{SP} is the work function of the spectrometer (3.70 eV) and E_{kin}^{0} is the on-set energy of secondary electron emission spectra (see Fig. 3(b)).

The areal densities of V_O were determined by ERD, which detected H^+(D^+) recoiled from the sample of interest exposed to $H_2{}^{16}O$($D_2{}^{18}O$) at ~330 K. We slightly heated the samples during water exposure in order to promote the desorption of water molecules non-reacted and produced via recombination of OH groups. Actually, temperature programmed desorption (TPD) measurements showed that H_2O desorption starts from RT and reaches a maximum rate at 350 K[15,16]. Here, we assumed that all the V_O vacancies were filled out by exposure to H_2O at ~330 K. Indeed, the STM observation showed that a V_O vacancy is quickly filled to form a paired $O_{br}H$ by H_2O exposure even in UHV (water background; ~10^{-11} Torr range) and even at a low

temperature of ~180 K[1,17,18]. It must be also noted that MEIS/ERD analysis performed for the *R*-TiO_2(110) exposed to $H_2{}^{18}O$ revealed that the H/^{18}O ratio was almost 2/1, as expected. Thus the number of V_O corresponds to just the half that of the detected H. It is also possible to estimate the areal density of O_{ad} by high-resolution MEIS for the sample exposed to $^{18}O_2$ at ~323 K down to RT. The scattering (recoil) yield $Y(\theta, E)$ is expressed by

$$Y(\theta, E) = Q\left(\frac{d\sigma}{d\Omega}\right) N\Delta x\ \Delta\Omega\ \varepsilon\ \eta_+, \qquad (2)$$

where θ, E, Q, and $\Delta\Omega$ are scattering (recoil) angle, scattered (recoiled) energy, number of incident ions, and solid angle subtended by a toroidal electrostatic analyzer, respectively. The $N\Delta x$ (atoms/cm^2) corresponds to the number (areal density) of target atoms of interest. Here, the value of $\Delta\Omega\cdot\varepsilon$ is 3.36×10^{-5}. The charge fractions (η_+) of scattered He^+ and recoiled H^+ ions, respectively were measured in advance using a thermally grown $Si^{18}O_2$ thin layer on a Si(001) substrate and a hydrogen-terminated Si(111)-1×1-H surface. We calculated the scattering/recoil cross sections, $\frac{d\sigma}{d\Omega}$ using the ZBL potentials[19] and estimated the energy spread of MEIS/ERD spectra employing the Lindhard-Scharff formula for energy straggling[20]. The uncertainties in the H and ^{18}O detection were ±0.5 and $\pm0.4\times10^{13}$ atoms/cm^2, respectively, which were roughly estimated from reproducibility (two or three times) and statistics for signal areas including the uncertainty of background levels. In order to avoid the radiation damage effects such as hydrogen escape from surfaces, the Ne^+ beam current was limited below 2 nA and the irradiated area was shifted slightly after accumulation of 0.5 and 0.05 μC for He^+ and Ne^+ impacts, respectively. Note that all the analysis measurements were made at RT. Further details can be found in the literatures[21,22].

3. Results and Discussion

Initially as-supplied TiO_2(110) substrates were annealed at 973 K for 30 min in UHV to be conductive owing to creation of Ti(Ti^{3+}) interstitials acting as an electron donor. Figure 2(a) shows the sheet resistance measured by the 4-point probe as a function of number of 0.75 keV Ar^+-sputtering/annealing (870 K for 5 min) cycles for the TiO_2(110) substrates purchased from companies S and F. The quite different initial values of sheet resistance are probably due to different crystal growth treatments. With increasing the number of sputter/annealing cycle, the sheet resistance is decreased

gradually and saturated at ~100Ω/□. The decreased sheet resistance with increasing the sputtering/annealing cycles is likely caused by an increase in the Ti-int density. Indeed, it was reported that the major diffusive species is Ti^{3+} interstitials at temperatures above 700 K by Henderson[23] using isotopically labeled ^{18}O and ^{46}Ti and also by Aono and Hasiguti[24] on the basis of electron-paramagnetic resonance measurements. We measured the defect state intensity dependent on sheet resistance, as shown in Fig. 2(b). The spectra from the bottom to top correspond to the sheet resistance of 900 (point A in Fig. 2(a)), 250 (point B), and 100 Ω/□ (point C). It is clearly seen that lower resistance gives higher defect state intensity. It is reasonable that the higher density of Ti-int in the bulk leads to a higher density of subsurface Ti-int by annealing in UHV. The sheet resistance changed from 900 to 250 Ω/□ resulted in reduction of the work function of ~0.2 eV (not shown here). There is a general trend that work function gradually decreases with decreasing the sheet resistance by continuing the sputtering/annealing cycles, although only a slight reduction was seen for the substrates subjected to sputtering/annealing cycles more than 5 times (see Fig. 2(a)).

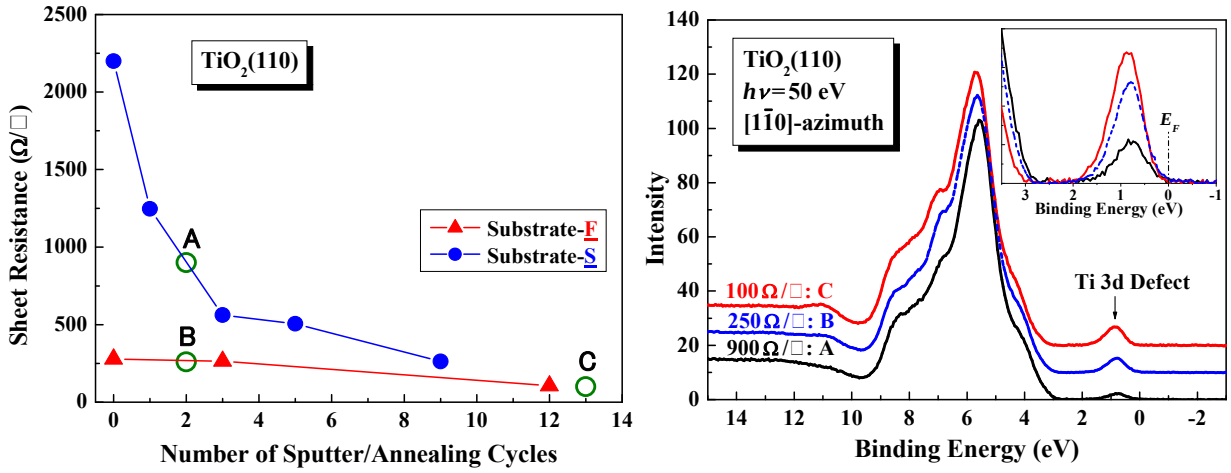

FIG. 2. (a) Sheet resistance measured by a 4-point probe for the TiO_2(110) substrates purchased from company S (circles) and F (triangles) as a function of sputter/annealing cycles. As-supplied substrates were initially annealed at 973 K for 30 min in UHV to be conductive. (b) UPS spectra taken at photon energy of 50 eV under normal emission condition ([1$\bar{1}$0]-azimuth) for TiO_2(110) substrates with sheet resistance of 900 (point A in (a)), 250 (point B), and 100 (point C) Ω/□ from bottom to top. Inset is magnified spectra around the defect state.

Next we prepared a nearly stoichiometric surface denoted by S^*-TiO_2 by annealing at 823 K in O_2 ambience (1×10^{-6} Torr) for 5 min. The sample was cooled down to RT keeping the same O_2 pressure. The TiO_2 substrates employed above and hereafter underwent the Ar^+-sputtering/annealing cycles more than 5 times in advance after the initial treatment to be conductive. According to Diebold[6], annealing R-TiO_2(110) surfaces in an O_2 ambience causes extraction of Ti-int atoms from the bulk and near-surface region to form added-layers of TiO_2(110) sometimes a partially incomplete surface structure such as Ti_2O_3-like (Ti-rich) clusters. The resulting surface structure depends mainly on the annealing temperature, the O_2 pressure, and the crystal reduction state. A Ti-rich surface with adstrucures was characterized by a broad O 2p feature in UPS spectra and a broad surface peak with a low energy tail for the scattering components from ^{16}O and Ti in MEIS spectra. We found out an optimum condition to form the nearly stoichiometric surface as described above by checking the RHEED patterns and UPS and MEIS spectra. Figure 3(a) shows the UPS spectra taken at a photon energy of 50 eV for the S^*-TiO_2(110), that annealed at 870 K for 10 min in UHV denoted by R^*-TiO_2(110), and R-TiO_2(110) subjected to 0.75 keV Ar^+-sputter/annealing cycles and finished by annealing at 870 K for 10 min in UHV. Strong defect state intensities appeared for both the R- and R^*-TiO_2(110), while only slightly seen the defect state peak for the S^*-TiO_2. Interestingly, a higher binding energy (E_B) shift of the valence band edge is seen only for the R-TiO_2(110) relative to those for the S^*- and R^*-TiO_2(110) (see the inset of Fig. 3(a): magnified spectra). This higher E_B shift (~0.3 eV) for the R-TiO_2(110) indicates a local downward band bending due to a surface dipole with a positive polarity on the vacuum side, which is induced by V_O creation because an O_{br} escapes from the surface as a neutral and the residual charge is partly given to underlying Ti atoms (Ti^{4+}). The fact that no significant E_B shift was seen for the R^*-TiO_2 in comparison with that for the S^*-TiO_2 suggests no significant V_O creation by annealing only (below 870 K for 10 min). This is confirmed by work function measurement. Figure 3(b) shows the secondary electron emission spectra for R-, S^*-, and R^*-TiO_2(110), where the samples were negatively biased at –6.45 V. The spectra give the work function of the R-TiO_2(110) smaller than those for the S^*- and R^*-TiO_2 by ~0.4±0.05 eV. This lower work function is consistent with the higher E_B shift (~0.3 eV) for R-TiO_2 relative to that for S^*-TiO_2, caused by V_O creation, which generates a surface dipole with a positive polarity on the vacuum side. Therefore, the gap state seen for the R^*-TiO_2(110) comes primarily from the Ti-int not

from V_O. Here, we must note that the S^*-TiO_2 has still a small amount of V_O (~0.5×10^{13} atoms/cm^2: ~0.01 ML), which was detected by H_2O exposure followed by ERD analysis. Some attention should be also paid to the fact that work function of TiO_2(110) tends to decrease gradually with decrease in sheet resistance. This sometimes degrades the reproducibility of work function measurements. Onda et al.[25] reported that the work function measured by two-photon photoemission technique for nearly stoichiometric TiO_2(110) ranged from 5.5 - 5.8 eV with an uncertainty of 0.3 eV owing to variability in the surface preparation. This large scatter may be caused by the treatment of annealing at 900 K in an O_2 pressure of 3×10^{-7} Torr for 40 min, which is different from the present condition.

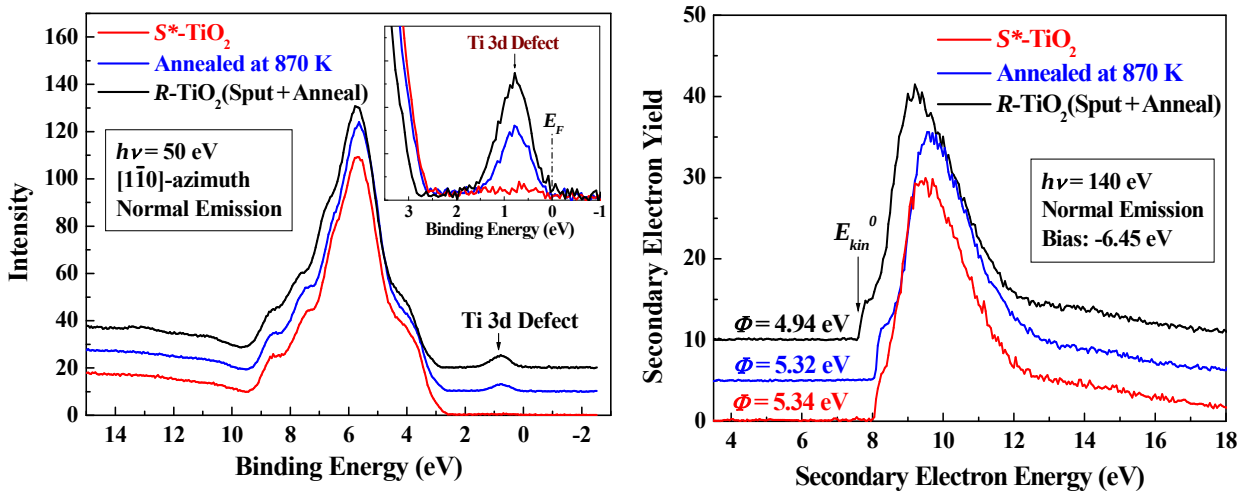

FIG. 3. (a) UPS spectra observed for S^*-TiO_2(110), R^*-TiO_2, and R-TiO_2(110) subjected to sputter/annealing and finished by annealing at 870 K for 10 min. The inset is magnified spectra around the gap state. The sheet resistance of the substrates were 100 - 200 Ω/□.
(b) Secondary electrons emitted by 140 eV photon incidence from S^*-, R^*-, and R-TiO_2(110).

In order to confirm the above interpretation, we exposed the R-TiO_2(110) and R^*-TiO_2(110) to $D_2{}^{18}O$ at 330 K and measured the areal densities of ^{18}O and D by MEIS and ERD, respectively. Figure 4(a) shows the MEIS spectra around the scattering component from ^{18}O observed for 80 keV He^+ ions incident on R- and R^*-TiO_2(110) substrates after $D_2{}^{18}O$ exposure of 100 L. The areal densities of ^{18}O are derived to be $3.7\pm0.4\times10^{13}$ atoms/cm^2 and less than 1×10^{13} atoms/cm^2, respectively. The former value corresponds to V_O concentration of 0.079 ML (1 ML = 5.2×10^{14} atoms/cm^2) after correction of $D_2{}^{18}O/H_2{}^{16}O$ ratio of 9/1. The recoiled D^+ spectra are

indicated in Fig. 4(b), which were measured by 80.66 keV Ne^+ impact at incident and emerging angles of 45° and 85°, respectively. The densities of D on the *R*- and *R**-TiO_2(110) surfaces, respectively are deduced to be 8.0±0.5 and 2.3±0.5×10^{13} atoms/cm^2. The former value is almost twice that of ^{18}O detected above. The results obtained clearly show that the V_O concentration for the *R**-TiO_2(110) prepared by annealing in UHV only for the nearly stoichiometric surface is ~1/4 compared with that for the *R*-TiO_2(110) formed by Ar^+-sputtering followed by the same annealing process. The V_O creation after the annealing only corresponds to 0.022 ML or less.

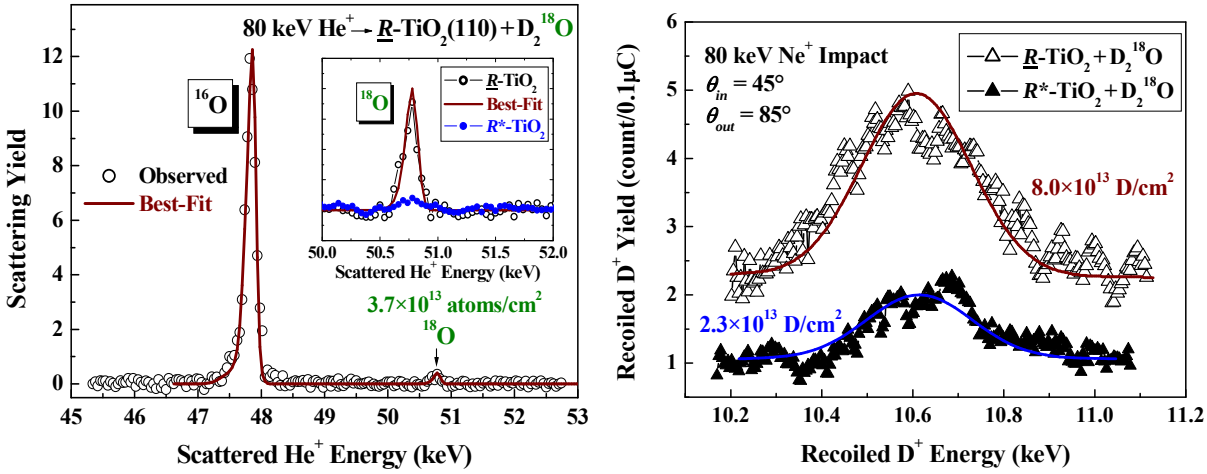

FIG. 4. (a) Observed (after 10 point smoothing) and best-fitted MEIS spectra for 80 keV He^+ ions incident along [100]-axis and scattered to [010]-axis of *R*-TiO_2(110) after $D_2{}^{18}O$ exposure of 100 L. Inset indicates magnified spectra around scattering component from ^{18}O for *R*-TiO_2(110) (open circles) and *R**-TiO_2(110) (full circles) after $D_2{}^{18}O$ exposure. (b) ERD spectra (after 10 point smoothing) observed for 80.66 keV Ne^+ impact on *R*-TiO_2(110) (open triangles) and *R**-TiO_2(110) (full triangles) after $D_2{}^{18}O$ exposureof 100 L. Recoiled D^+ spectra were best-fitted by symmetric Gaussian profiles (solid curves).

Diebold et al.[26,27] observed by STM nearly stoichiometric TiO_2(110) surfaces annealed at temperatures above 700 K and found creation of V_O. However, the density of V_O was probably a few % (0.01 - 0.03 ML) on average over a wide range, which is much smaller than that observed for the *R*-TiO_2(110) prepared by Ar^+-sputter/annealing cycles (0.08 - 0.10 ML). Sputtering/annealing cycles in UHV create V_O more efficiently rather than annealing only. It must be also noted that the exact mechanism of V_O creation is still not known[28].

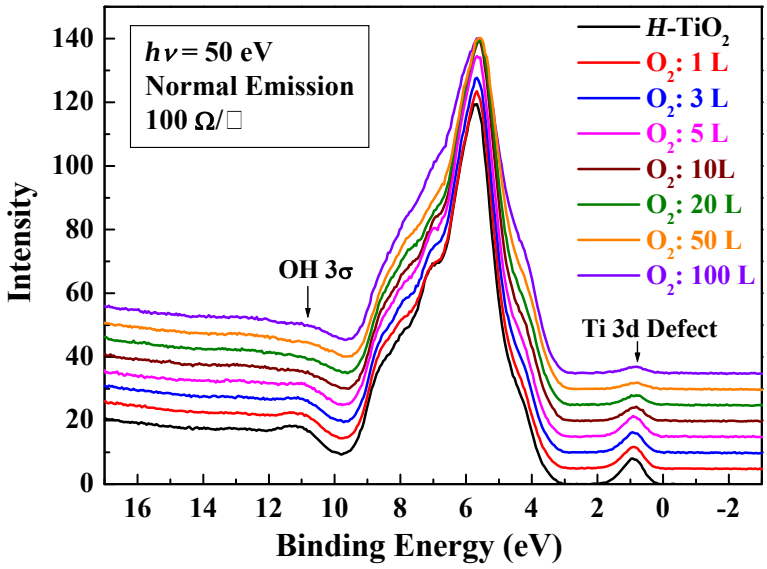

FIG. 5. UPS spectra observed for H-TiO_2(110) exposed to O_2 at RT as a function of O_2 dose.

As mentioned before, Wendt et al.[1] reported that exposing an H-TiO_2(110) surface with paired $O_{br}H$ to an O_2 gas led to complete disappearance of OH 3σ signal but still kept a strong gap state intensity at a low O_2 exposure, indicating existence of a subsurface excess charge different from V_O. We checked the intensities of the Ti 3d defect state and OH 3σ appearing around ~0.8 and ~11 eV below the E_F, respectively for H-TiO_2(110) exposed to O_2 at RT. Figure 5 shows the UPS spectra measured for H-TiO_2(110) and that after O_2 dose, as a function of O_2 exposure. The TiO_2 substrate used here had a sheet resistance of ~100 Ω/□. The intensities of Ti 3d and OH 3σ normalized by those for the H-TiO_2(110) are plotted as a function of O_2 exposure for the substrates with sheet resistance of ~100 (Fig. 6(a)) and ~900 (Fig. 6(b)) Ω/□. Here, the open and filled symbols denote the photon incidence of 50 and 90 eV, respectively. For the TiO_2 substrate with a lower sheet resistance (~100 Ω/□, 15 cycles), the normalized defect state intensity still keeps a value of ~0.5 at O_2 exposure of 10 L, whereas the OH 3σ intensity drops to 0. The residual defect state intensity originates from Ti-int. This trend is similar to the result reported by Wendt et al.[1]. In contrast, the residual defect state intensity is small when the OH 3σ signal disappeared at 50 L for the substrate with a higher resistance (900Ω/□, 2 cycles). In any cases, after O_2 exposure above 100 L, the Ti 3d defect state intensity remained at ~0.2. Such a gap state intensity remained was also observed by Wendt et al.[1] and Yim et al.[3]. This

probably comes from the Ti-int (Ti^{3+}) located in a relatively deep subsurface region, which cannot deliver the excess charge to allow for O_{ad} atom creation but can emerge as photoemission, although limited to an escape depth.

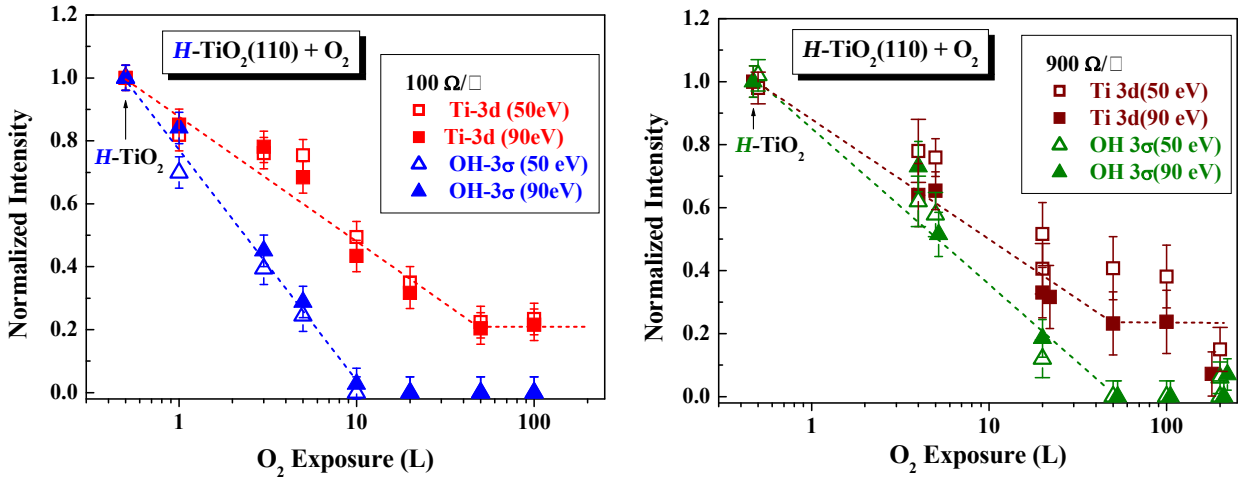

FIG. 6. Normalized intensities of Ti 3d defect state (squares) and OH 3σ (triangles) signals, as a function of O_2 dose for the substrates with sheet resistance of 100 Ω/□ (a) and with 900 Ω/□ (b). Filled and open symbols denote incident photon energy of 50 and 90 eV, respectively.

Finally, we estimate the electronic excess charge (δ_V) when a V_O is created in other word the charge to heal the V_O. Here, the electronic charge withdrawn by an O_{ad} atom (δ_A) is assumed to be 0.8 e, which was predicted by Wendt et al.[1] based on the first principle calculations. It is possible to derive the absolute amounts (areal densities) of V_O for R-TiO_2(110) and of unfilled V_O after exposing the R-TiO_2(110) to O_2 at 330 K - RT (denoted by O-TiO_2(110)) by detecting the H for the R- and O-TiO_2(110) exposed to H_2O (10 L) at 330 K, because all the V_O vacancies are quickly filled to form $O_{br}H$ pairs[1,17,18]. The density of V_O corresponds to just the half that of the detected H, as mentioned before. Figures 7(a) and (b) indicate the ERD spectra observed for the R- and O-TiO_2(110) exposed to H_2O (10 L) at 330 K and the densities of H adsorbed are deduced to be $1.10\pm0.05\times10^{14}$ and $5.9\pm0.5\times10^{13}$ atoms/cm^2, respectively and thus the densities of V_O correspond to the half, namely 5.5 (n_V: ~0.11 ML), and 3.0×10^{13} atoms/cm^2 (~0.06 ML). The latter (n_V') corresponds to the areal density of V_O unfilled after O_2 exposure. The density of O atoms adsorbed was derived to be $5.8\pm0.4\times10^{13}$ atoms/cm^2 by detecting ^{18}O by MEIS for the R-TiO_2(110) exposed to $^{18}O_2$ (2000 L) at RT, as shown in Fig. 7(c), where the scattering components from ^{16}O and ^{18}O are

observed separately. The narrow peak without a low energy tail for the scattering component from ^{16}O suggests no Ti-rich oxides clusters on the surface. After correction of $^{18}O/^{16}O$ ratio of 95/5 in the exposure gas, the density of O (n_O) adsorbed in V_O vacancies partly and 5-fold Ti rows is determined to be $6.1\pm0.4\times10^{13}$ atoms/cm^2.

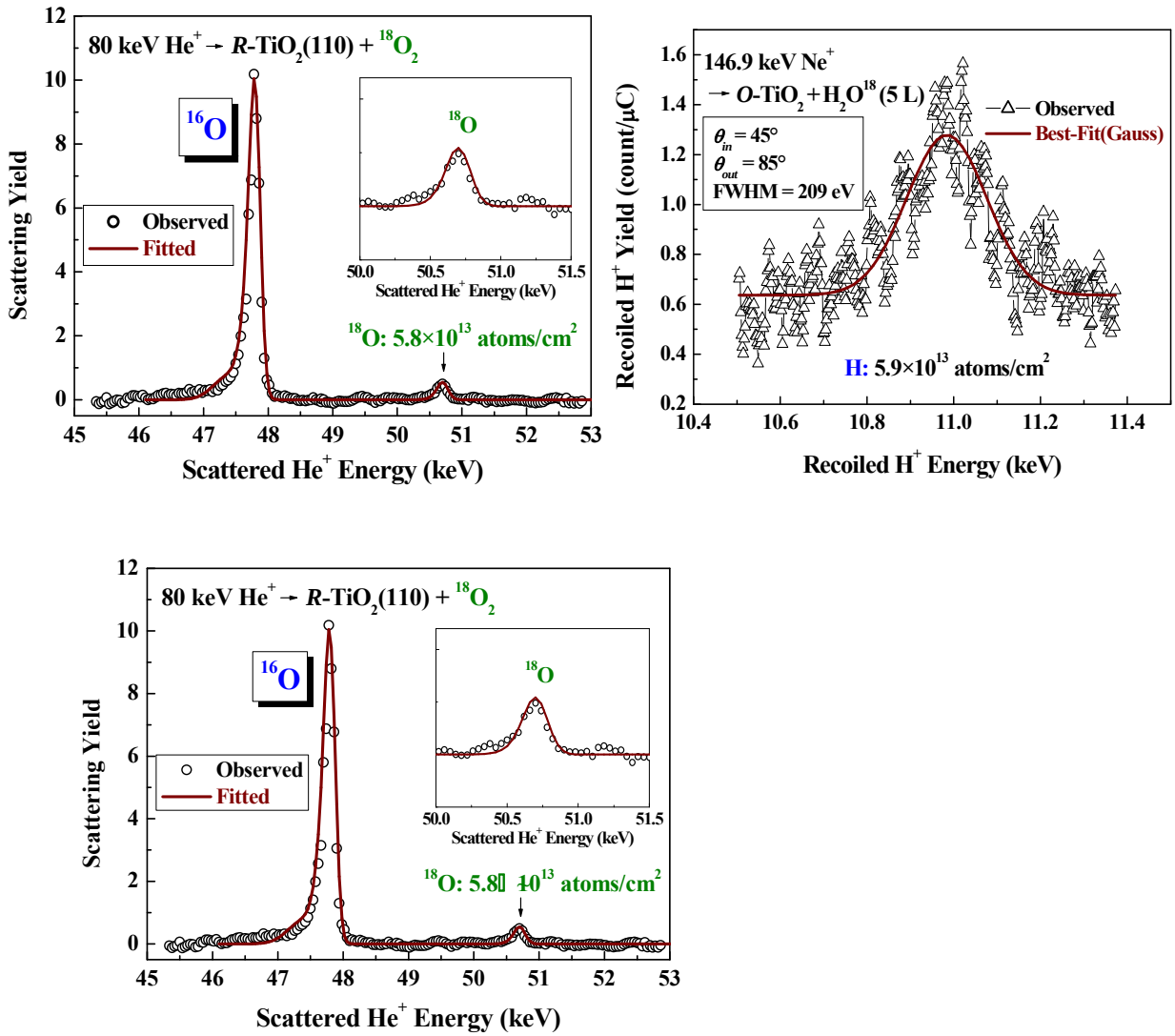

FIG. 7. ERD spectra observed at 147 keV Ne^+ impact for (a) R-TiO_2(110) and (b) O-TiO_2(110) after H_2O exposure of 10 L. (c) MEIS spectrum (circles) observed using 80 keV He^+ ions for R-TiO_2(110) exposed to $^{18}O_2$. The inset is the magnified spectrum around the scattering signal from ^{18}O. The sheet resistances of the substrates are 100 - 200 Ω/□.

As the results, we obtain the following equation,

$$0.8\ e\cdot\{n_O-(n_V-n_V')\}+\delta_V\cdot(n_V-n_V')=k\cdot(I_{R-TiO}\ -\ I_{O-TiO}),\qquad(3)$$

where $n_V-n_V'=(5.5-3.0)\times10^{13}$ corresponds to the areal density of V_O filled after O_2 exposure and thus $n_O-(n_V-n_V')$ is the density of O_{ad} atoms adsorbed in the 5-fold Ti rows. As the result, the value of $[\{n_O-(n_V-n_V')\}-n_V']=0.60\times10^{13}$ atoms/cm^2 is the excess O atoms (~0.01 ML) on the *O*-TiO_2(110) surface. The defect state intensity (*I*) in the UPS spectra was normalized by the spectrum height in the E_B range from 13 to 15 eV. Here, the I_{R-TiO} and I_{O-TiO}, respectively are the normalized defect state intensity for the *R*- and *O*-TiO_2(110) and k is an appropriate coefficient to convert the defect state intensity to an electronic charge. In order to determine the δ_V value, we need one more equation. We observed UPS and MEIS spectra for ^{16}*O*-TiO_2(110) exposed to CO (12000 L) and then dosed with $^{18}O_2$ at RT. It was evidenced previously that O_{ad} atoms react with CO to form CO_2[29]. Therefore, the number of detected ^{18}O atoms (after ^{18}O/^{16}O correction) coincides with that of the O_{ad} atoms reacted with CO. Figure 8(a) shows the UPS spectra observed for *O*-TiO_2(110) after exposed to CO (12000 L) and then dosed with O_2 (2000 L). The corresponding MEIS spectrum observed for the *O*-TiO_2(110) exposed to CO and then dosed with $^{18}O_2$ is indicated in Fig.8(b). The areal density of the adsorbed O atoms on the 5-fold Ti for the substrate exposed to CO followed by $^{18}O_2$ dose is estimated to be 3.4±0.4×10^{13} atoms/cm^2 after correction of ^{18}O/^{16}O ratio of 95/5. We measured three times the MEIS spectra subsequently for the *O*-TiO_2(110) under almost the same treatment because of the small ^{18}O yield. As the results, the average density (n_A) of the adsorbed O atoms on the 5-fold Ti after the above treatment is deduced to be 3.1±0.4×10^{13} atoms/cm^2. Correlating the O adsorption on the 5-fold Ti, the defect state intensity is decreased, almost extinct (see Fig. 8(a)) because O_{ad} atoms (electronegative species) withdraw subsurface excess charge from underlying Ti^{3+}. We now obtain the second equation given by

$$0.8\ e\cdot n_A=k\cdot(I_{CO}\ -\ I_{CO-O}),\qquad(4)$$

where I_{CO} and I_{CO-O}, respectively are the normalized defect state intensities for the *O*-TiO_2(110) after CO exposure of 12000 L and that further dosed with O_2 (2000L). Inputting (see Table I) the n_O= 6.1±0.4×10^{13}, n_V= 5.5±0.5×10^{13}, n_V'= 3.0±0.5×10^{13}

atoms/cm^2, and the observed defect state intensities normalized, I_{CO} = 28±4, I_{CO-O} = 3±2, I_{R-TiO} = 81±5, and I_{O-TiO} = 15±3 deduces the δ_V value of 1.45±0.2 e, which is significantly larger than the δ_A value of 0.8 e [1]. Note that different first principle calculations gave similar δ_A values of 0.9 e [4] and 0.7 e [30]. Importantly, the fact that the electronic charge to heal a V_O is almost twice that withdrawn by an O_{ad} means more stable O_{br} energetically than O_{ad}. Indeed, O_{ad} atoms readily react with CO molecules to form CO_2 at room temperature[29,31]. In addition, the present result is consistent with the clear image of excess charge of V_O distributed symmetrically on multiple 5-fold Ti^{4+} sites observed by STM[11] and also with sharing of a V_O charge by neighboring 5-and 6-fold Ti atoms extracted from resonant photoelectron diffraction[12].

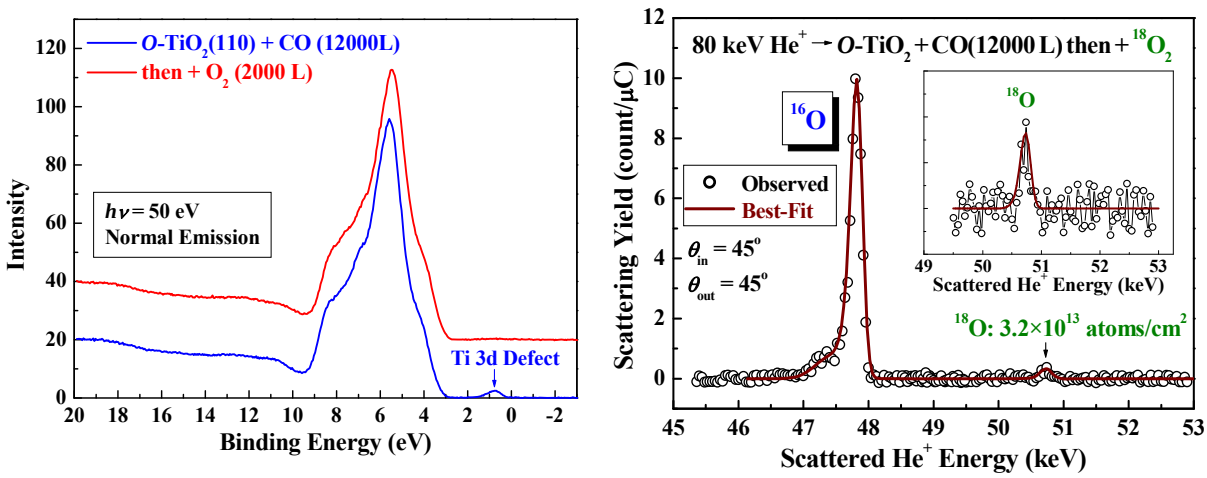

FIG. 8 (a) UPS spectra observed for ^{16}O-TiO_2(110) exposed to CO (12000 L) (bottom) and then dosed with $^{18}O_2$ (2000 L) (top). (b) MEIS spectrum observed for ^{16}O-TiO_2(110) exposed to CO (12000 L) and then dosed with $^{18}O_2$ (2000 L). The inset indicates the magnified spectrum around the scattering signal from ^{18}O. The substrates used here have sheet resistance of 100 - 200 Ω/□.

Table I. Areal densities of V_O and adsorbed O as well as normalized defect state intensities (I) for R-TiO_2(110) and that after O_2 exposure (2000 L) and for O-TiO_2(110) after CO exposure (12000 L) followed by O_2 dose (2000 L). Correction of isotopic fraction ($^{18}O/^{16}O$ = 9/1) was made for density of adsorbed O. The unit of the areal density is ×10^{13} atoms/cm^2.

	R-TiO_2	O-TiO_2	O-TiO_2 after CO exposure	O-TiO_2 after CO exposure and then dosed with O_2
Density of V_O	n_V : 5.5±0.5	n_V' : 3.0±0.5		

Density of adsorbed O		n_O : 6.1±0.4		n_A : 3.1±0.4
Normalized defect state intensity	81±5	15±3	28±4	3±2

Using the charges provided by a V_O (1.45*e*) and a Ti-interstitial (0.8*e*), we estimate roughly the contribution from Ti-int from the results shown in Fig. 3(a). The gap state intensity ratio of the *R*-TiO_2 to *R**-TiO_2 is approximately 2/1 and the V_O ratio of *R*-TiO_2 to *R**-TiO_2 is ~4/1. It is reasonable to assume a same contribution (*x* ML) to the gap state from Ti-int for both samples. As the result, the following equation is obtained,

$$\frac{2}{1} = \frac{1.45\ e \cdot 0.079 + 0.8\ e \cdot x}{1.45\ e \cdot 0.079 / 4 + 0.8\ e \cdot x}. \tag{5}$$

Here, the V_O density of 7.9 % (0.079 ML) for *R*-TiO_2 is used, which was determined by $D_2{}^{18}O$ exposure as mentioned before. Thus we obtain the density of ~7 % (0.07 ML) for the Ti-int condensed near the surface and contributing to the gap state. This value is comparable with that (0.05 - 0.06 ML) predicted by Wendt et al.[1]. Obviously, V_O is the primary source for *R*-TiO_2, whereas Ti interstitials become dominant for *R**-TiO_2.

4. Conclusion

The present study clearly shows the followings: (i) The intensity of the gap state is well correlated with the sheet resistance of the substrate employed, inversely proportional to the density of the subsurface Ti-int. (ii) Sputter/annealing cycles in UHV creates V_O and condenses the subsurface Ti-int, while only annealing below 870 K does not create V_O significantly. (iii) The electronic charge to heal a V_O corresponding to the charge delivered to underlying Ti atoms by a V_O creation is almost twice (~1.45±0.2 *e*) that withdrawn by an O_{ad} (0.8 *e*: given by the first principles calculations). This fact clearly explains less stable O_{ad} than O_{br}, in other word, more reactive O_{ad} than O_{br}. It is also concluded that both the V_O and Ti-interstitials condensed near the surface region contribute to the gap state and the contribution from the Ti-int becomes comparable to that from V_O for the substrates with a low sheet resistance less than ~200 Ω/□. There is a general trend that the increase in subsurface Ti interstitials leads to gradual reduction of work function.

Acknowledgement

The authors would like to thank our colleagues, F. Matsuda and M. Tagami for their experimental assistant. This work was partly supported by subsides from Japan Science and Technology Agency, JST, ‘CREST’ and also from Ministry of Education, Japan, ‘Academic Frontier Project’.

References

[1] S. Wendt, P.T. Sprunger, E. Lira, G.K.H. Madsen, Z. Li, J.Ø. Hansen, J. Matthiesen, A. Blekinge-Rasmussen, E. Lægsgaard, B. Hammer, and F. Besenbacher, Science **320**, 1755 (2008).

[2] N.G. Petrik, Z.Zhang, Y. Du, Z. Dohnálek, I. Lyubinetsky, and G.A. Kimmel, J. Phys. Chem. **C 113**, 12407 (2009).

[3] C.M. Yim, C.L. Pang, and G. Thornton, Phys. Rev. Lett. **104**, 036806 (2010).

[4] A.C. Papageorgiou, N.S. Beglitis, C.L. Pang, G. Teobaldi, G. Cabailh, Q. Chen, A.J. Fisher, W.A. Hofer, and G. Thornton, PNAS **9**, 2391 (2010).

[5] S. Wendt, R. Bechstein, S. Porsgaard, E. Lira, J.Ø. Hansen, P. Huo, Z. Li, B. Hammer, and F. Besenbacher, Phys. Rev. Lett. **104**, 259703 (2010).

[6] U. Diebold, Surf. Sci. Rep. **48**, 53(2003).

[7] C. Di Valentin, G. Pacchioni, and A. Selloni, Phys. Rev. Lett. **97**, 166803 (2006).

[8] B.J. Morgan and G.W. Watson, Surf. Sci. **601**,5034 (2007).

[9] R.L. Kurtz, R. Stockbauer, T.E. Madey, E. Román, and J.L. de Segovia, Surf. Sci. **218**, 178 (1989).

[10] Z. Zhang, S-P. Jeng, and V.E. Henrich, Phys. Rev. **B 43**, 12004 (1991).

[11] T. Minato, Y. Sainoo, Y. Kim, H.S. Kato, K. Aika, M. Kawai, J. Zhao, H. Petek, T. Huang, W. He, B. Wang, Z. Wang, Y. Zhao, J. Yang, and J.G. Hou, J. Chem. Phys. **130**, 124502 (2009).

[12] P. Krüger, S. Bourgeois, B. Domenichini, H. Magnan, D. Chandesris, P.Le Fèvre, A.M. Flank, J. Jupille, L. Floreano, A. Cossaro, A. Verdini, and A. Morgante, Phys. Rev. Lett. **100**, 055501 (2008).

[13] E. Finazzi, C. Di Valentin, and G. Pacchioni, J. Phys. Chem. **C 113**, 3382 (2009).

[14] T. Okazawa, M. Kohyama, and Y. Kido, Surf. Sci. **600**, 4430 (2006).

[15] Z. Zhang, Y. Du, N.G. Petrik, G.A. Kimmel, I. Lyubinetsky, and Z. Dohnálek, J. Phys. Chem. **C 113**, 1908 (2009).

[16] M.A. Henderson, W.S. Epling, C.H.F. Peden, and C.L. Perkins, J. Phys. Chem. **B 107**, 534 (2003).

[17] S. Wendt, J. Matthiesen, R. Schaub, E.K. Vestergaard, E. Lægsgaard, F. Besenbacher, and B. Hammer, Phys. Rev. Lett. **96**, 066107 (2006).

[18] O. Bikondoa, C.L. Pang, R. Ithnin, C.A. Muryn, H. Onishi, and G. Thornton, Nature Mater. **5**, 189 (2006).

[19] J.F. Ziegler, J.P. Biersack and W. Littmark, *The Stopping and Range of Ions in Matter*, Pergamon, New York, 1985.
[20] J. Lindhard and M. Scharff, K. Dan. Vidensk. Selsk. Mat.-Fys. Medd. **27** (15) (1953).
[21] K. Mitsuhara, T. Matsuda, H. Okumura, A. Visikovskiy, and Y. Kido, Nucl. Instrum. Methods **B 269**, 1859 (2011).
[22] K. Mitsuhara, T. Kushida, H. Okumura, H. Matsumoto, A. Visikovskiy, and Y. Kido, Surf. Sci. **604**, L48 (2010).
[23] M.A. Henderson, Surf. Sci. **419**, 174 (1999).
[24] M. Aono and R.R. Hasiguti, Phys. Rev. **B 48**, 12406 (1993).
[25] K. Onda, B. Li, and H. Petek, Phys. Rev. **B 70**, 045415 (2004).
[26] U. Diebold, F. Anderson, K-On Ng, and D. Vanderbilt, Phys. Rev. Lett. **77**, 1322 (1996).
[27] J.-M. Pan, B.L. Maschhoff, U. Diebold, and T.E. Madey, J. Vac. Sci. Technol. **A 10**, 2470 (1992).
[28] Z. Dohnálek, I. Lyubinetsky, and R. Rousseau, Prog. Surf. Sci. **85**, 161 (2010).
[29] K. Mitsuhara, H. Okumura, A. Visikovskiy, M. Takizawa, and Y. Kido, Chem. Phys. Lett. **513**, 84 (2011).
[30] Y. Du, N.A. Deskins, Z. Zhang, Z. Dohnálek, M. Dupuis, and I. Lyubinetsky, Phys. Chem. Chem. Phys. **12**, 6337 (2010).
[31] Z. Wang, Y. Zhao, X. Cui, S. Tan, A. Zhao, B. Wang, and J. Yang, J. Phys. Chem. **C 114**, 18222 (2010).